Tailoring Medium-Entropy Alloys for Advanced Hydrogen Storage

Karel Saksl

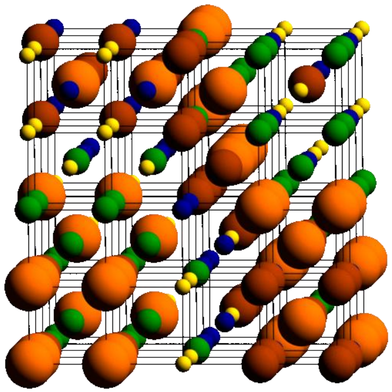

SjF

Outline

- *Introduction*

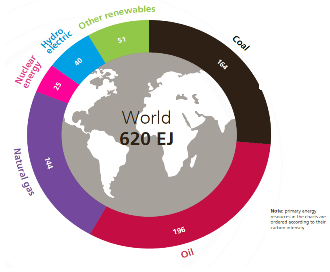

- *Tailoring the* $(TiVNb)_{85}Cr_{15}$ *alloy*
  - *alloying strategy*
  - *deformation strategy*

Word energy consumption in 2024

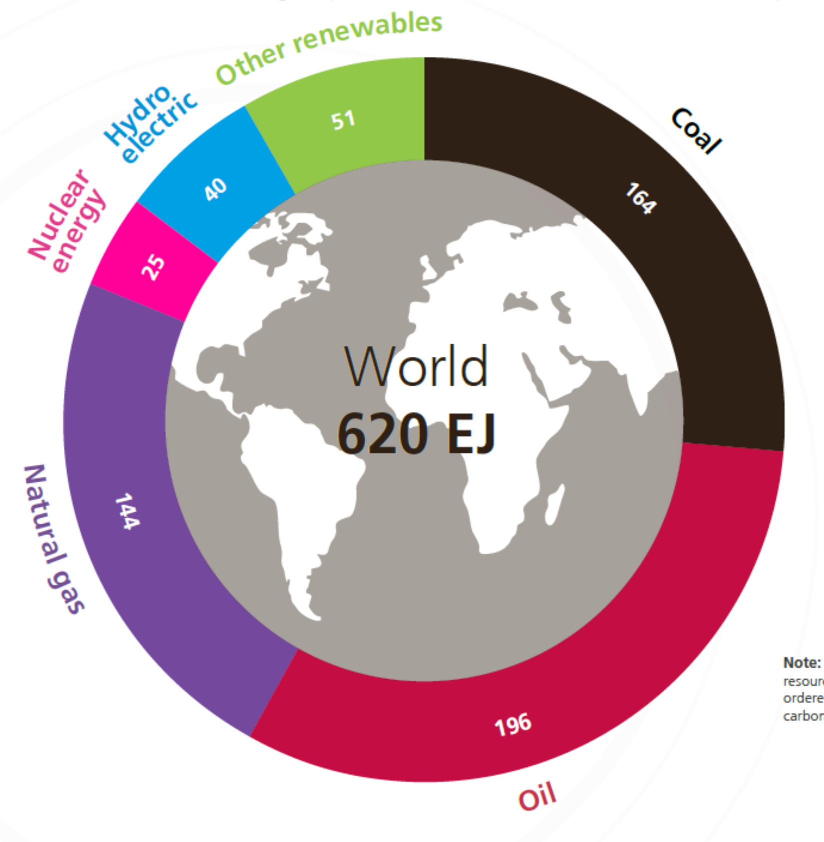

Fossil fuels accounting for 84% of the energy mix.

Note: primary energy resources in the charts are ordered according to their carbon intensity.

Energy Institute Statistical Review of World Energy 2024

Word energy consumption in 2024

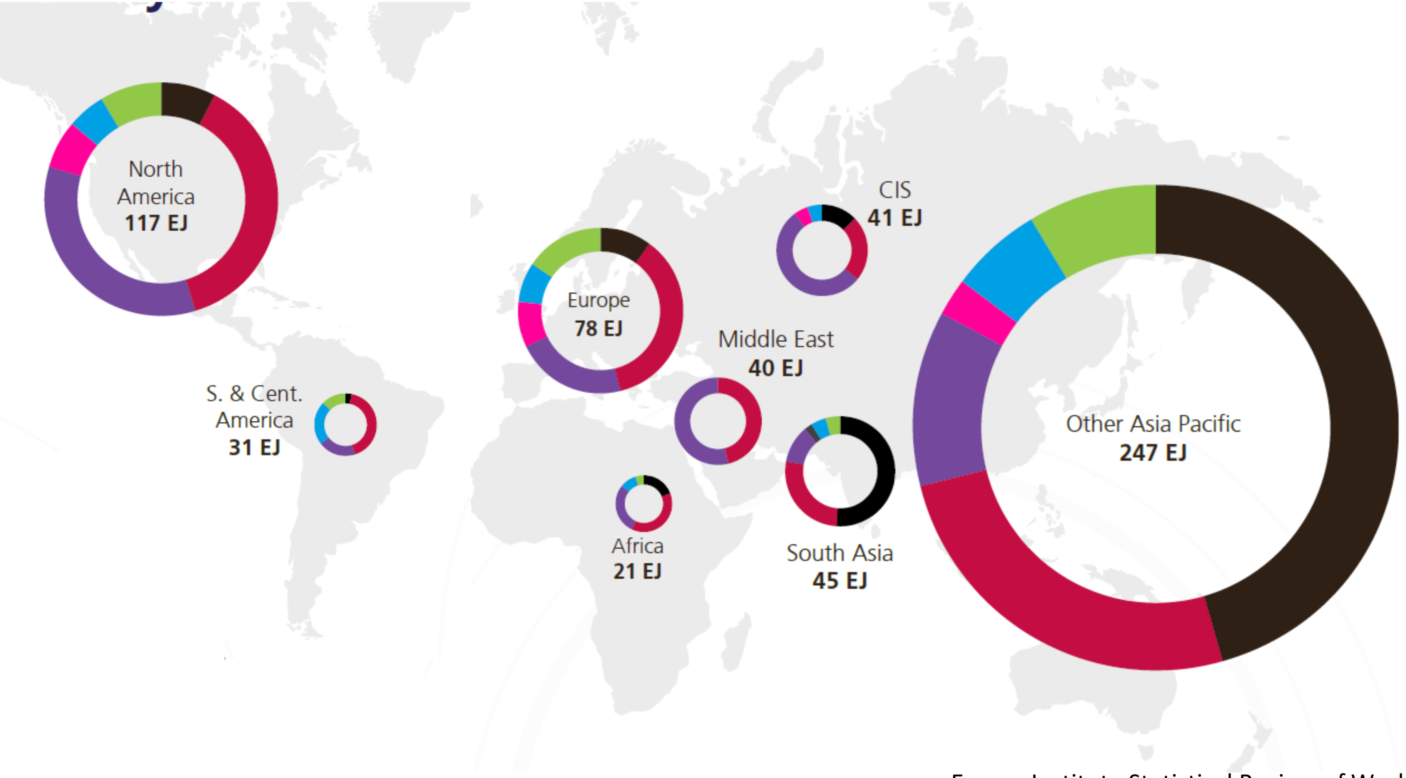

Energy Institute Statistical Review of World Energy 2025

Energy Storage, Hydrogen vs. Batteries

- **Batteries**, efficiency 85-95%
  low capacity. The largest battery storage
  Envision Jingyi Chagan Hada = 0.004 TWh

- **Hydrogen**, production efficiency 60-70%, re-generation of electricity with an efficiency of only 40-60%.

*The overall **electricity-to-hydrogen-to-electricity efficiency** is typically about **30–40%**, mainly due to losses during electrolysis, hydrogen compression/storage, and reconversion to electricity in the fuel cell.*

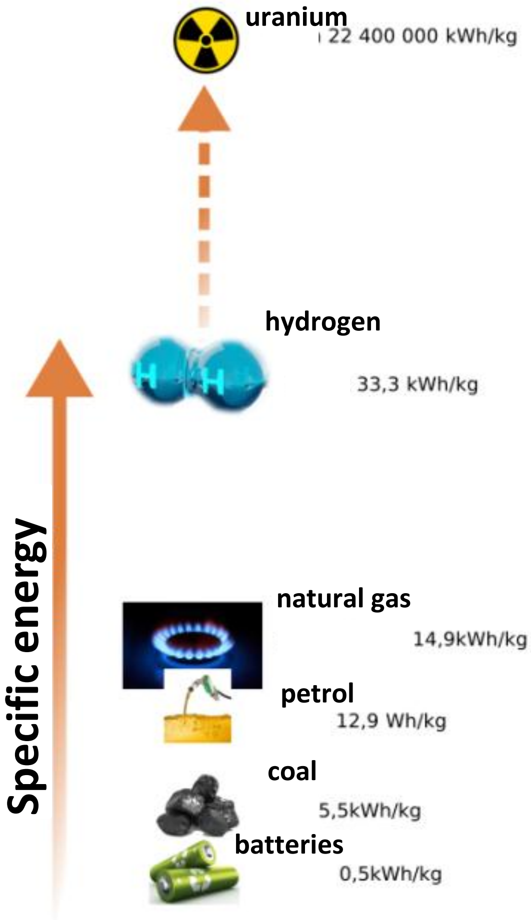

Energy supply

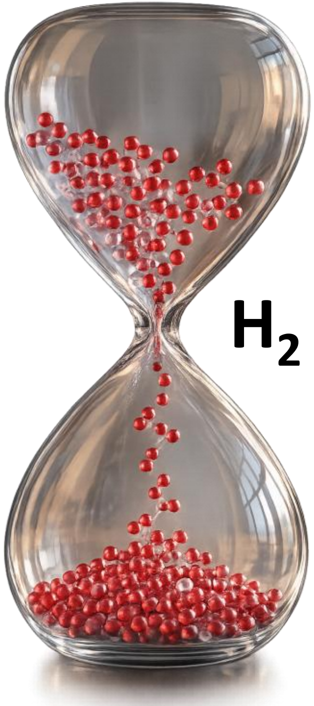

H_2 production

electrolysis of water
industrial by-product
from fossil fuels

H_2 storage & transport

H_2 utilization

traffic
power
industry
agriculture
medicine

End use

Efficient and secure storage/transport is critical for development of the hydrogen industry !

Hydrogen storage

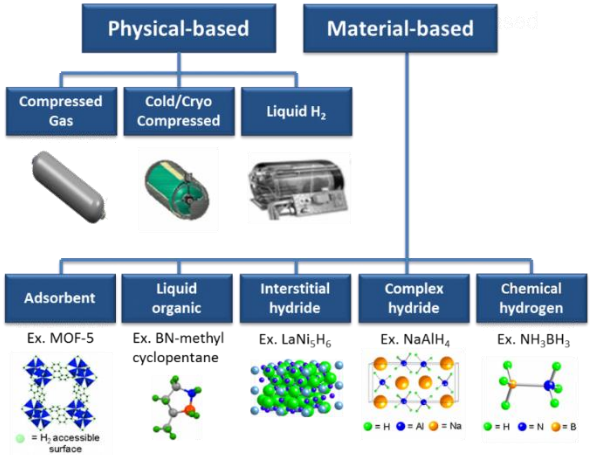

https://www.energy.gov/eere/fuelcells/hydrogen-storage

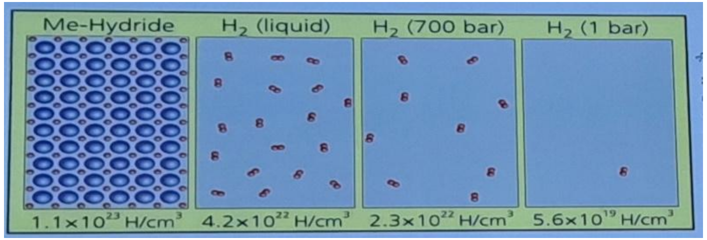

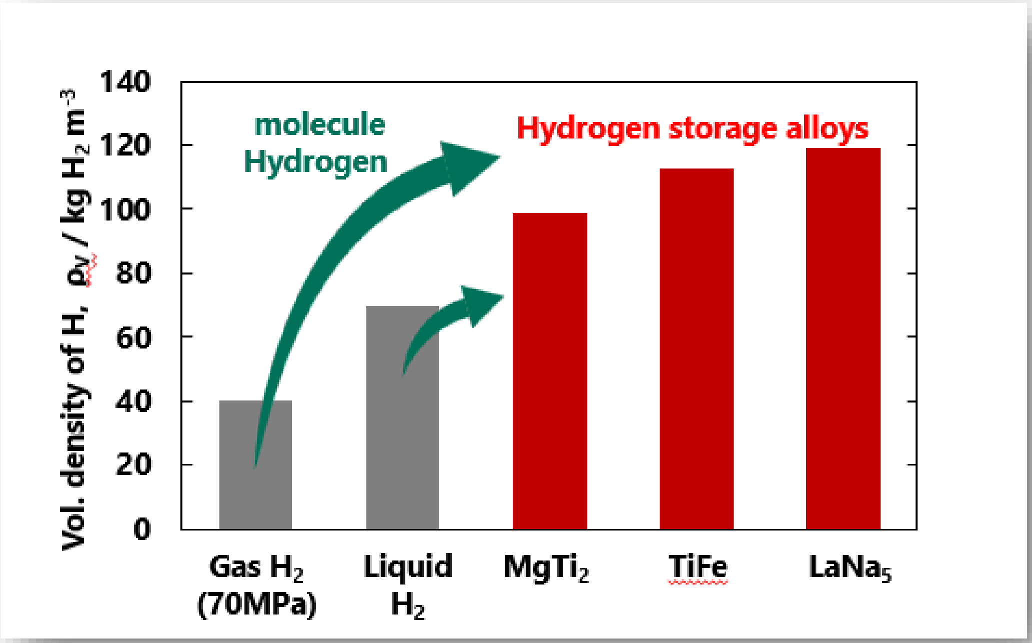

Züttel A., Mater. Today 6, 24 (2003).

Hydrogen storage

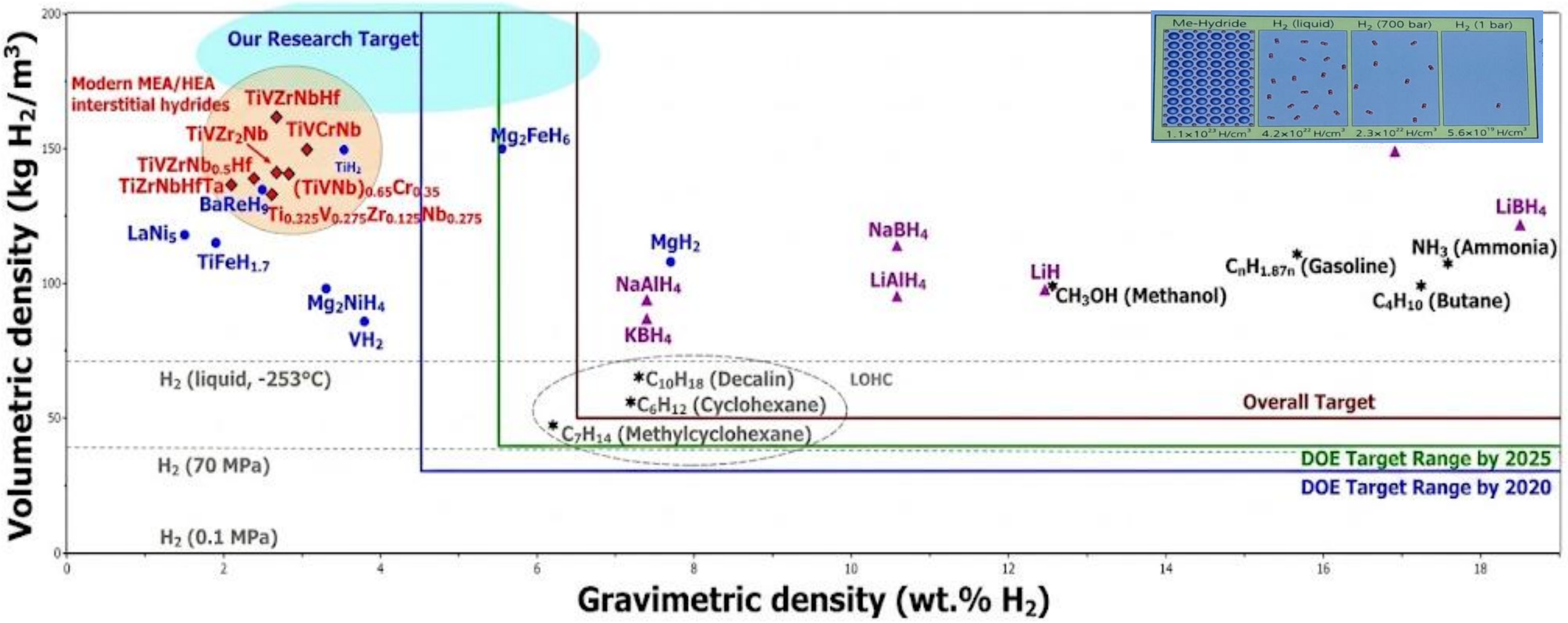

High-entropy alloys

Conventional alloy

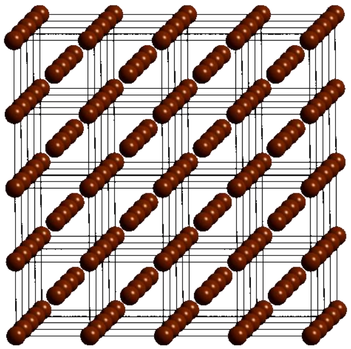

HEA

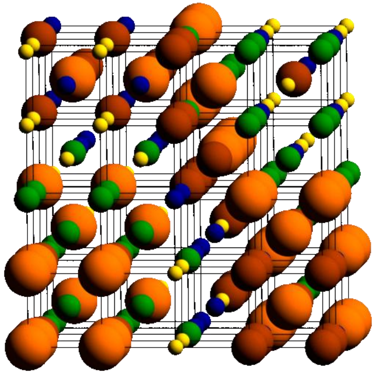

HEAs *were originally defined as a blend of 5 or more elements with concentrations between 5 and 35 atom percent, but the field now includes materials with as few as 3 principal elements, and where the maximum element concentration may be higher than 35 atom percent.*

High-entropy & hydrogen affinity

high mixing entropy (mainly configurational) in HEAs lowers the free energy of solid solution phases and facilitates their formation. Due to this enhanced mutual solubility among constituent elements, the number of phases present in HEAs can be evidently reduced.

$$\Delta G_{mix} = \Delta H_{mix} - T\Delta S_{mix}$$

<u>mixing enthalpy</u>

$$\Delta Hmix = \sum_{i=1, i\neq j}^{n} \omega_{ij} c_i c_j$$

while

$$\omega_{ij} = 4\Delta_{mix}^{AB}$$

<u>mixing entropy</u>

$$\Delta S_{mix} = -R\sum_{i=1}^{n} c_i \ln c_i$$

R - gas constant

<u>hydrogen affinity</u>

$$\Delta H_{\infty} = \sum_{i=1}^{n} c_i \Delta H_{\infty i}$$

$$\Delta H_f = \sum_{i=1}^{n} c_i \Delta H_{f i}$$

n – number of elements, c_i concentration of particular element in alloy.

ΔH_{Mix}^{AB}- mixing enthalpies of binary AB alloys*.

ΔH_{∞}- enthalpy of solution at infinite dilution

ΔH_f- enthalpy of formation of the concentrated hydride

* *A. Takeuchi, A. Inoue: Calculations of Mixing Enthalpy and Mismatch Entropy for Ternary Amorphous Alloys, Material Transactions, JIM, 11 (2000) 1372-1378*

Alloy Chemical Composition - **Strategy**

BCC structure is the most advantageous for high hydrogen uptake, as it has the most interstitial sites – a total of 18 sites comprised of 12 tetrahedral, and 6 octahedral sites which can be simultaneously occupied

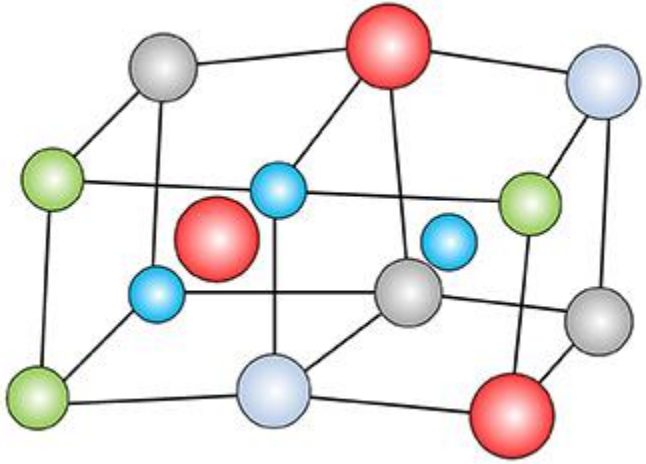

Parameter	**Requirement**
ΔS_{mix}	maximal
ΔH_{mix}	> -10 and < 5 kJ/mol
Ω	≥ 1.1
δ	≤ 6.6%
VEC	<4.75
ΔH_{∞} a ΔH_f	minimal

Tailoring the $(TiVNb)_{85}Cr_{15}$
- **alloying strategy**

Tailoring the $(TiVNb)_{85}Cr_{15}$ – alloying strategy

$(TiVNb)_{85-x}Cr_{15}Zr_x$, x = 1, 4 and 7

Table 1. Thermodynamic parameters of the alloy $(TiVNb)_{85}Cr_{15}$ and the alloys with Zr additions investigated.

Alloy	δ [%]	ΔH_{mix} [kJ·mol^{-1}]	Ω	ΔS_{mix} [J.K^{-1}.mol^{-1}]	T_m [K]	*VEC*
Precursor $(TiVNb)_{85}Cr_{15}$	5.76	−3.04	8.37	1.36 *R*	2257	4.87
Zr1 $(TiVNb)_{84}Cr_{15}Zr_1$	5.96	−3.07	8.54	1.40 *R*	2255	4.86
Zr4 $(TiVNb)_{81}Cr_{15}Zr_4$	6.48	−3.17	8.70	1.47 *R*	2251	4.84
Zr7 $(TiVNb)_{78}Cr_{15}Zr_7$	6.93	−3.27	8.69	1.52 *R*	2246	4.82

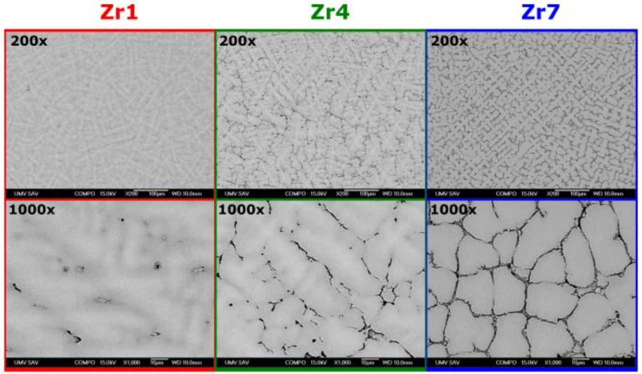

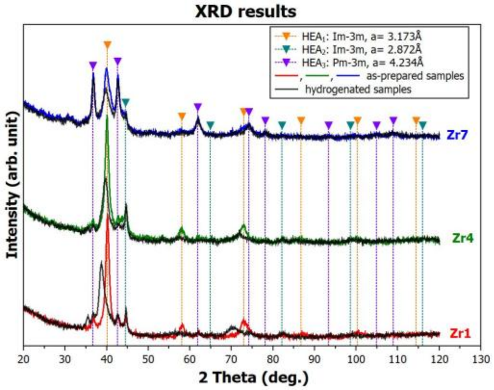

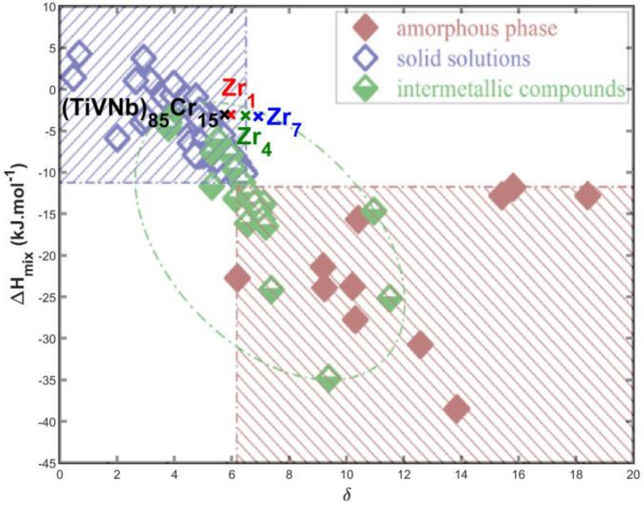

Saksl, K.; Matvija, M.; Fujda, M.; Ballóková, B.; Varcholová, D.; Kubaško, J.; Möllmer, J.; Lange, M.; Podobová, M. Zirconium-Modified Medium-Entropy Alloy $(TiVNb)_{85}Cr_{15}$ for Hydrogen Storage. *Materials* **2024**, *17*, 1732. https://doi.org/10.3390/ma17081732

Tailoring the $(TiVNb)_{85}Cr_{15}$ – alloying strategy

$(TiVNb)_{85-x}Cr_{15}Zr_x$, x = **1**, **4** and **7**

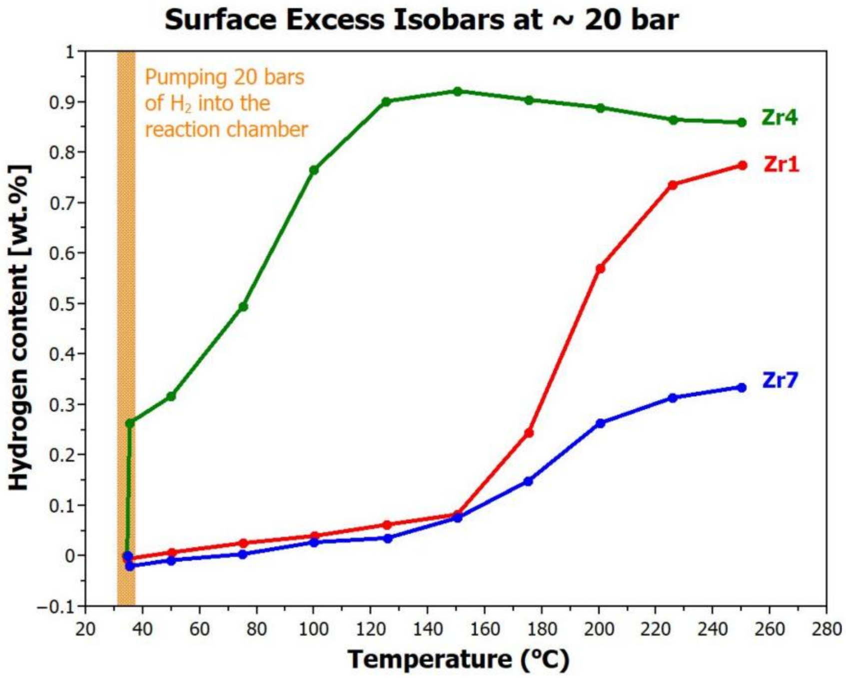

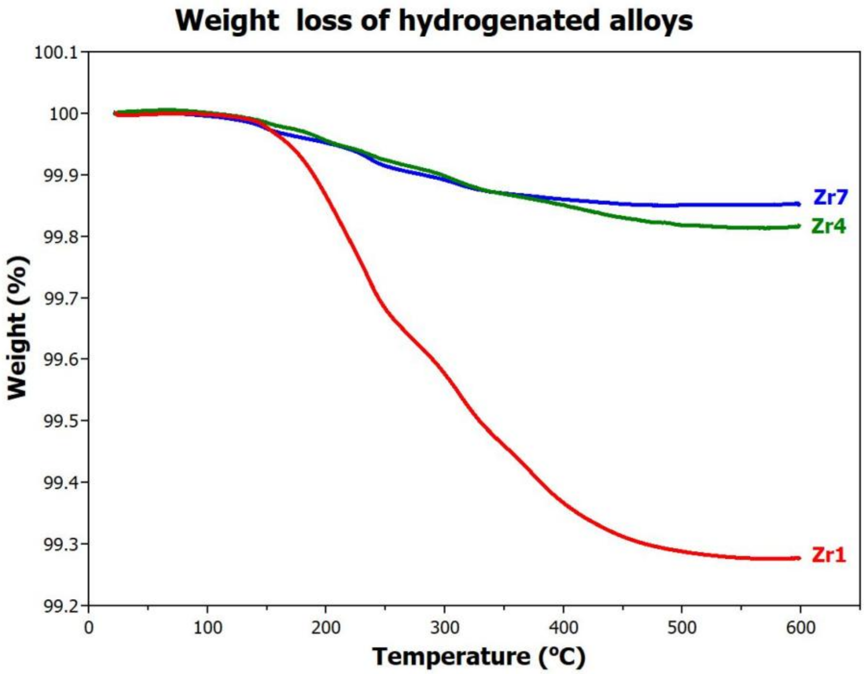

Saksl, K.; Matvija, M.; Fujda, M.; Ballóková, B.; Varcholová, D.; Kubaško, J.; Möllmer, J.; Lange, M.; Podobová, M. Zirconium-Modified Medium-Entropy Alloy $(TiVNb)_{85}Cr_{15}$ for Hydrogen Storage. *Materials* **2024**, *17*, 1732. https://doi.org/10.3390/ma17081732

Tailoring the $(TiVNb)_{85}Cr_{15}$ - **deformation strategy**

Tailoring the $(TiVNb)_{85}Cr_{15}$ – deformation strategy

High Pressure Torsion

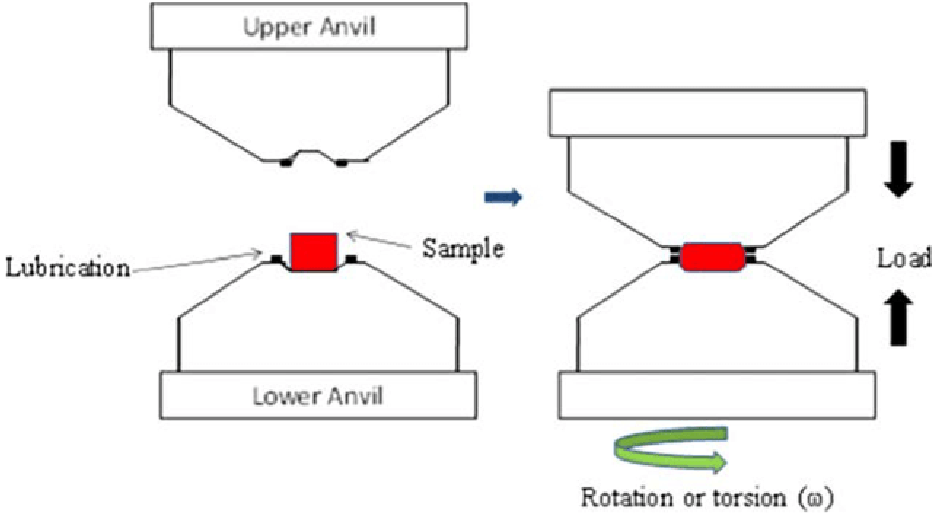

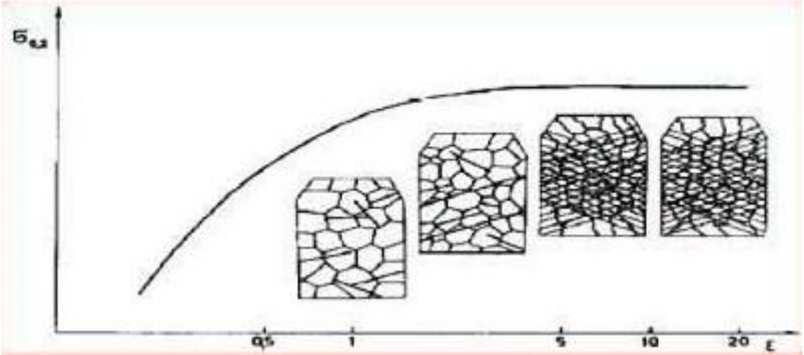

Tatsuya Ueda, Shuhei Yoshida, Shivam Dangwal, Łukasz Gondek, Kazuhiro Fukami, Ludmila Kučerová, Karel Saksl, Kaveh Edalati, Nobuhiro Tsuji,
Effect of lattice defects on hydrogen storage properties of HfNbTiZr medium entropy alloy,
International Journal of Hydrogen Energy, 155, 2025, https://doi.org/10.1016/j.ijhydene.2025.150292.

Material $(TiNbV)_{85}Cr_{15}$

Processing: Arc-melting -> homogenized at 1200°C for 24h + water quenching

Microstructure: BCC single phase. Density: 6.55 g/cm^3

Microstructure of as-cast specimen [BCC single phase] ↑Solidification direction

SEM-BSE SEM-EDX Element distribution (Identical area)

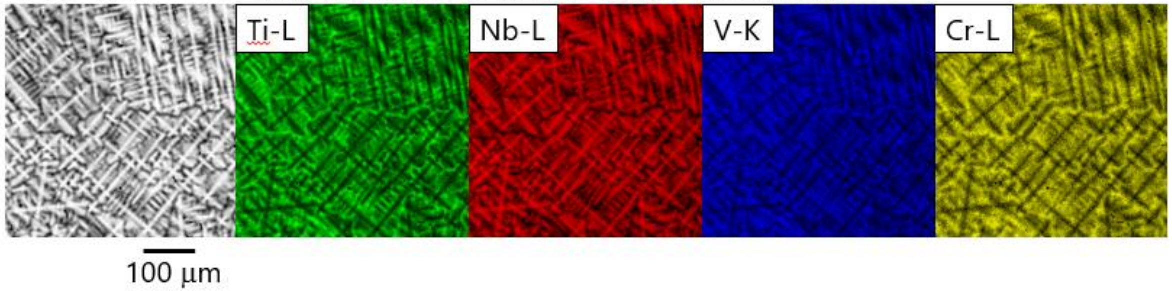

Microstructure of homogenized (1200 °C-24h) specimen [BCC single phase]

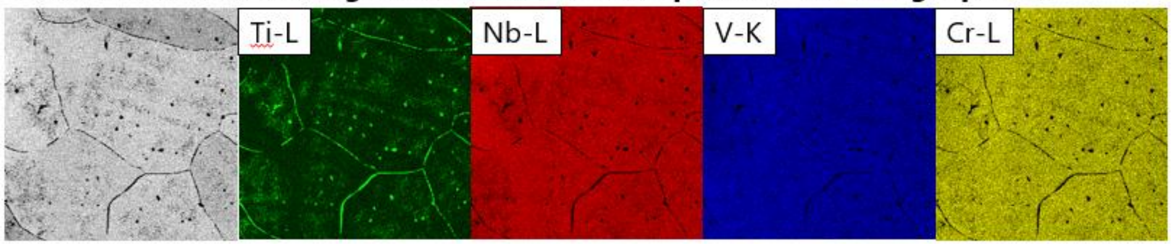

100 µm

Elemental segregation was almost eliminated by homogenization.
Ti tends to remain along grain boundaries.

Material

Processing: HPT 7.5GPa, 0.2 RPM, 5 rotations at room temperature. Max. shear strain 196.

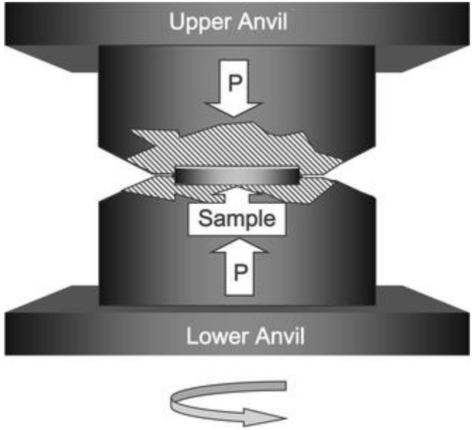

$(TiNbV)_{85}Cr_{15}$

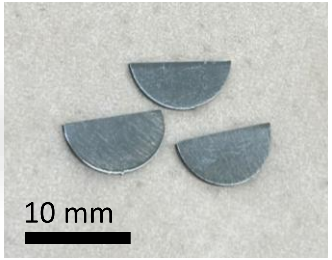

Bright-field STEM image (High mag.)

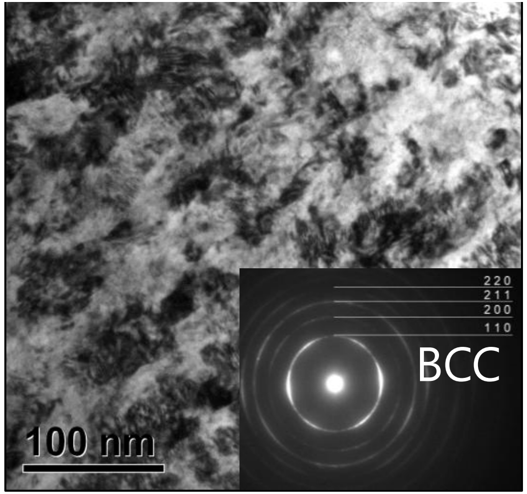

Microstructure: BCC single phase nanocrystalline structure with a mean grain size of **20-50 nm**, **about 10 times smaller than in conventional BCC metals and alloys**, Density: 6.55 g/cm^3

Hydrogenation Kinetics in $(TiNbV)_{85}Cr_{15}$

Activation procedures

(Reducing surface oxides on specimen surface → Hydrogen can easily react with materials)

Condition: Room temperature, Hydrogen pressure of ~3.5MPa, 20h

↓

Hydrogenation kinetics tests at 423K (150 °C) under hydrogen pressure of ~3.5MPa, up to **3h (180min)**

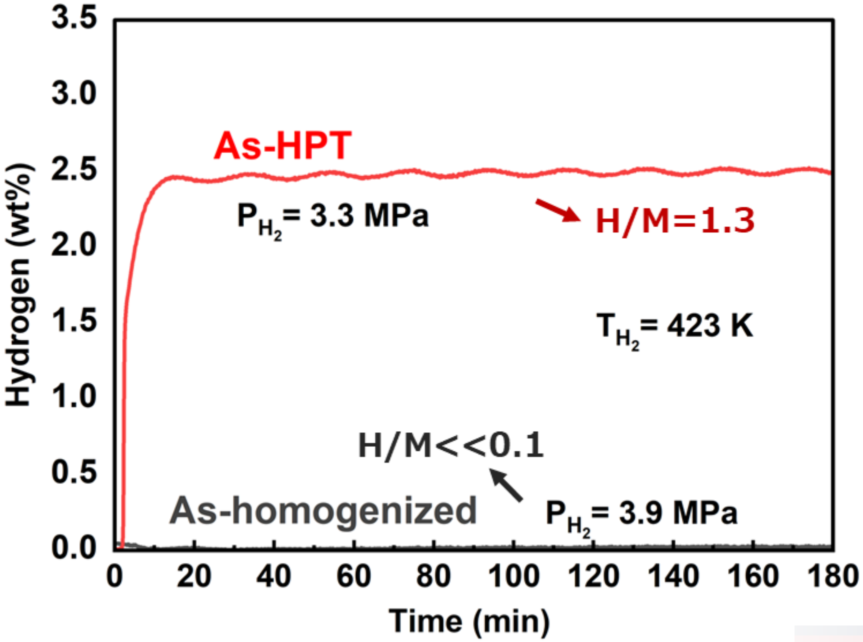

Specimen shape before hydrogenation

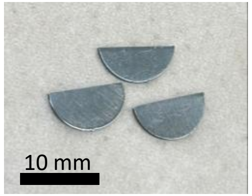

Specimen shape after hydrogenation

Homogenized **HPT-processed**

Maintained the shape

Became powders

Hydrogenation Kinetics in $(TiNbV)_{0.85}Cr_{0.15}$

Activation procedures

(Reducing surface oxides on specimen surface → Hydrogen can easily react with materials)

Condition: Room temperature, Hydrogen pressure of ~3.5MPa, 20h

↓

Hydrogenation kinetics tests (Test #2)

at 150 ^{o}C under hydrogen pressure of ~3.5MPa, up to **20h (1200min)**

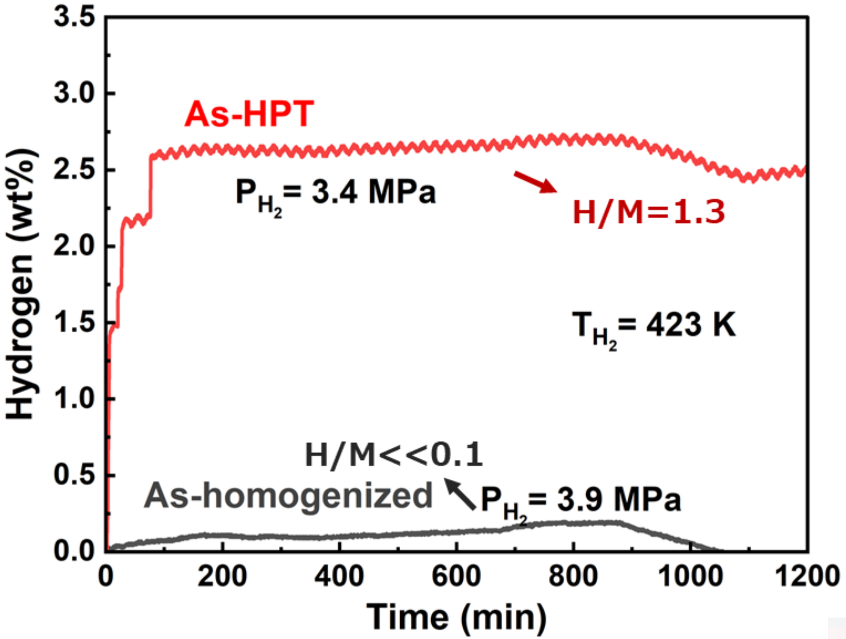

As-HPT specimen absorbed more hydrogen within shorter periods compared to the as-homogenized specimen

⇩

Hydrogenation kinetics was enhanced by introducing high density lattice defects through HPT process

Phase Transformation in Hydrogenation

Before hydrogenation

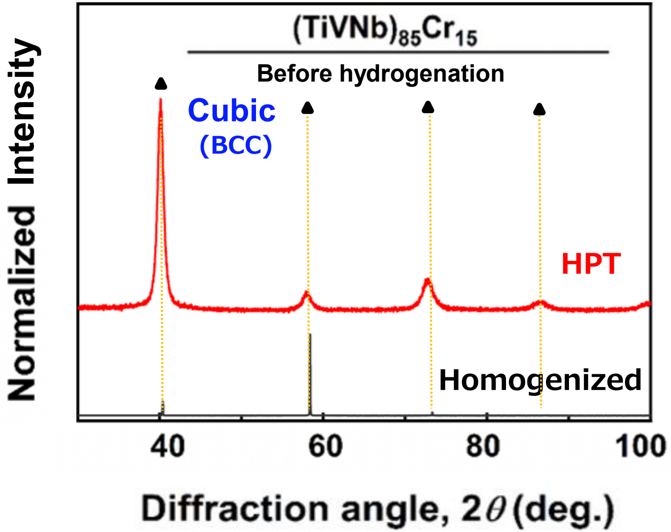

After 20h hydrogenation

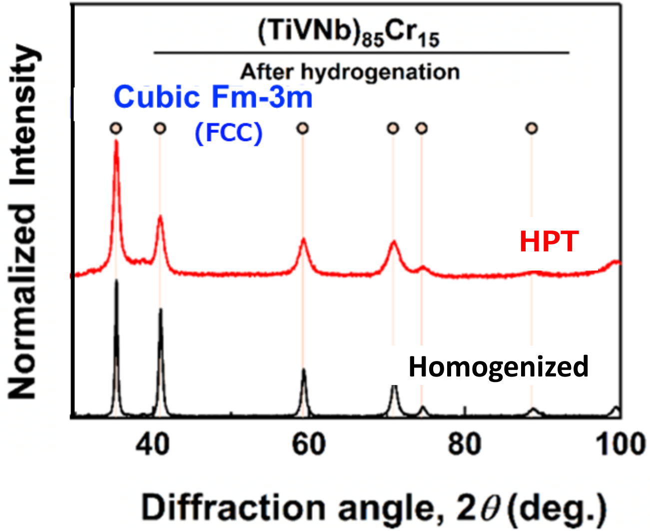

Phase transformation from BCC to FCC phase occurred during hydrogenation.

Hydride phase with an FCC structure formed.

Our goal and intention

hydrogen absorption storage and compressor

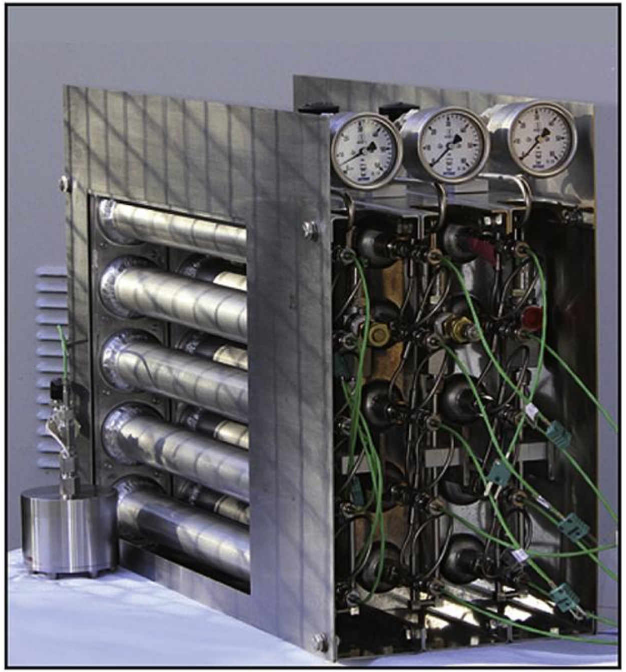

Challenges in metalhydrides development

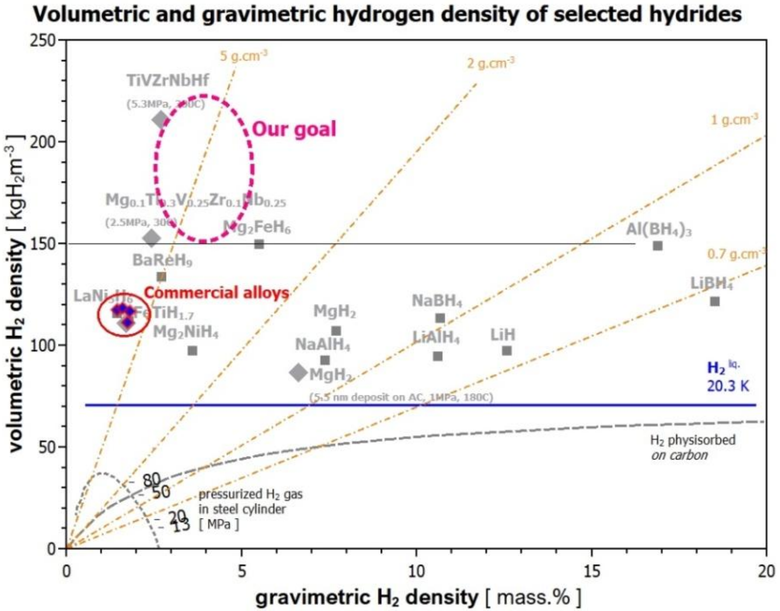

"Target Explanation Document: Onboard Hydrogen Storage forLight-Duty Fuel Cell Vehicles" (PDF). US Department of Energy. Archived (PDF) from the original on Apr 11, 2021.

Parameter	Current level „state-of-the-art“	Our goal
H/M ratio	1	>2
Mass energy content	1.4-1.8%	>2.5%
Volumetric energy density	0.04 kg/l	>0.15 kg/l
Hydrogen desorption temperature	20-300 °C	<130°C (onset) <160°C (peak)
Hydrogen desorption kinetics from the alloy containing 4-10 kg H_2	1.1 g/s	>1.6 g/s
Cyclic stability of the alloy	>1000	>1200 cycles with possibility of regeneration
The price of the alloy	5000 €/kg H_2	<3500 €/kg of stored H_2

Fundamental understaning

Synchrotron research

Diamond Light Source UK

PETRA III Germany

ESRF France

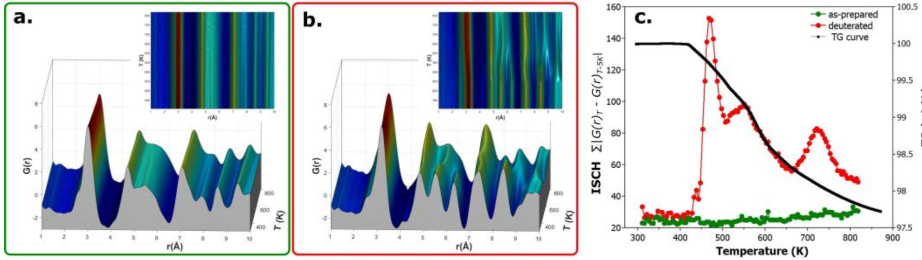

Fundamental understaning

Neutron research

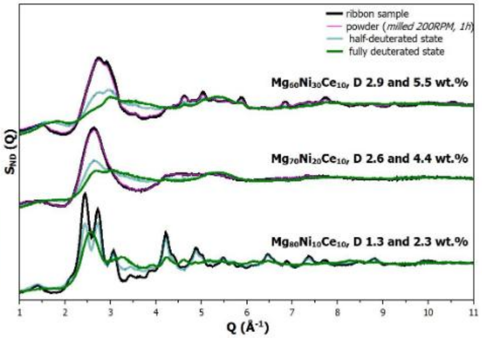

Fundamental understaning

Free electron laser research

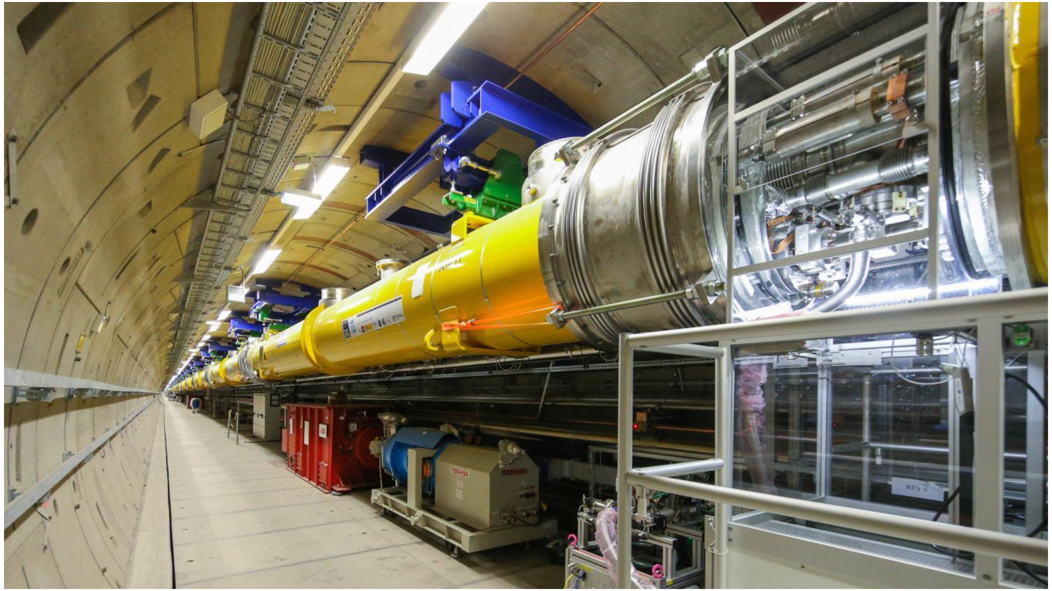

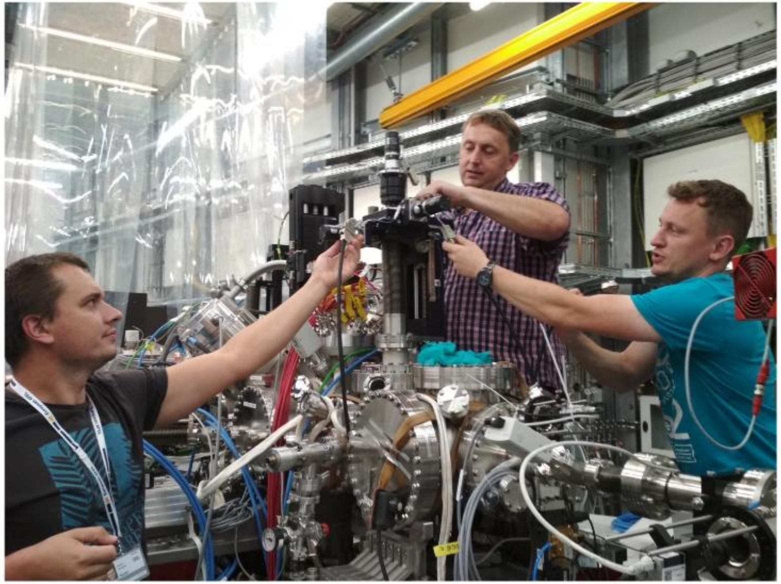

Acknowledgement

Strojnícka fakulta

INC

AGH

PRÍRODOVEDECKÁ FAKULTA UNIVERZITY P. J. ŠAFÁRIKA V KOŠICIACH • 1963 •

wigner

ZÁPADOČESKÁ UNIVERZITA V PLZNI

DESY

ill NEUTRONS FOR SCIENCE

BNC Budapest Neutron Centre

MINISTERSTVO ŠKOLSTVA, VEDY, VÝSKUMU A ŠPORTU SLOVENSKEJ REPUBLIKY

PROMATECH VÝSKUMNÉ CENTRUM PROGRESÍVNYCH MATERIÁLOV A TECHNOLÓGIÍ

APVV

Humphry Davy 1810 with hydrogen and oxygen

Thank you for your attention

SOLAR RESOURCE MAP

PHOTOVOLTAIC POWER POTENTIAL

WORLD BANK GROUP ESMAP SOLARGIS

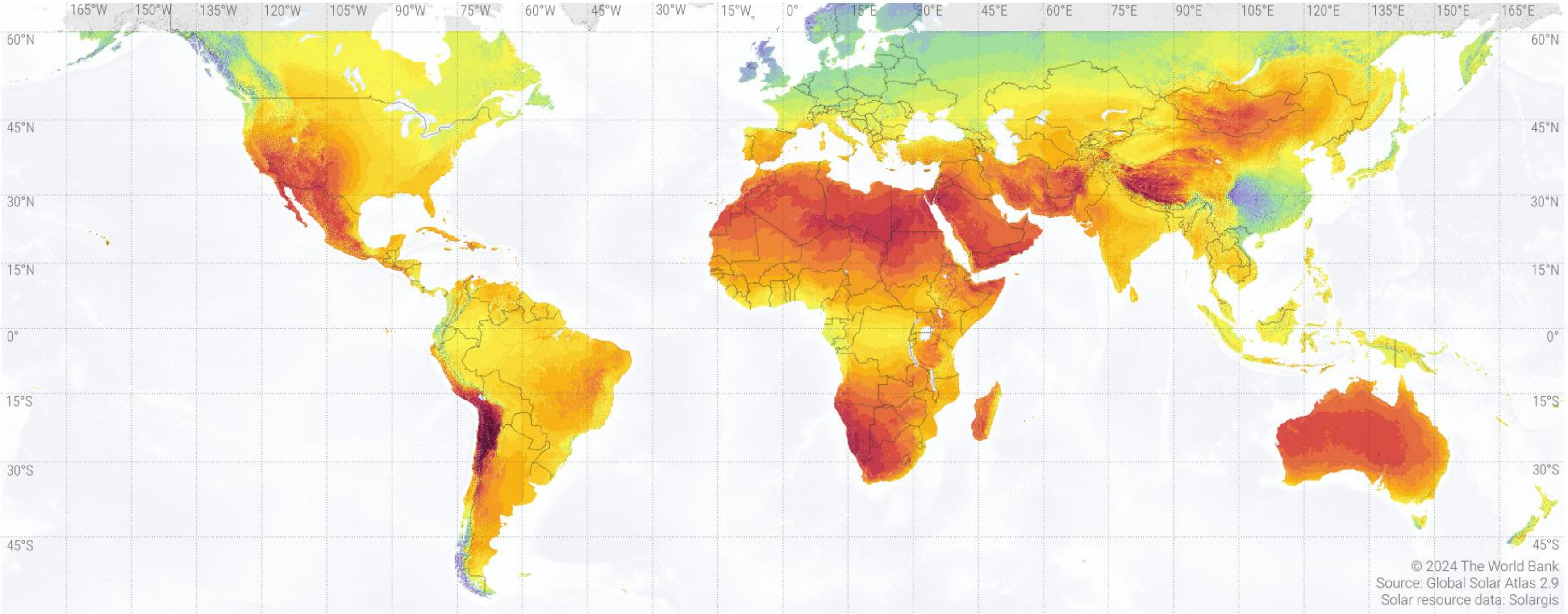

Long-term average of photovolaic power potential (PVOUT)

Daily totals:	2.0	2.4	2.8	3.2	3.6	4.0	4.4	4.8	5.2	5.6	6.0	6.4	kWh/kWp
Yearly totals:	730	876	1022	1168	1314	1461	1607	1753	1899	2045	2191	2337	

This map is published by the World Bank Group, funded by ESMAP, and prepared by Solargis. For more information and terms of use, please visit http://globalsolaratlas.info.

ONSHORE & OFFSHORE WIND RESOURCE MAP

WIND POWER DENSITY POTENTIAL

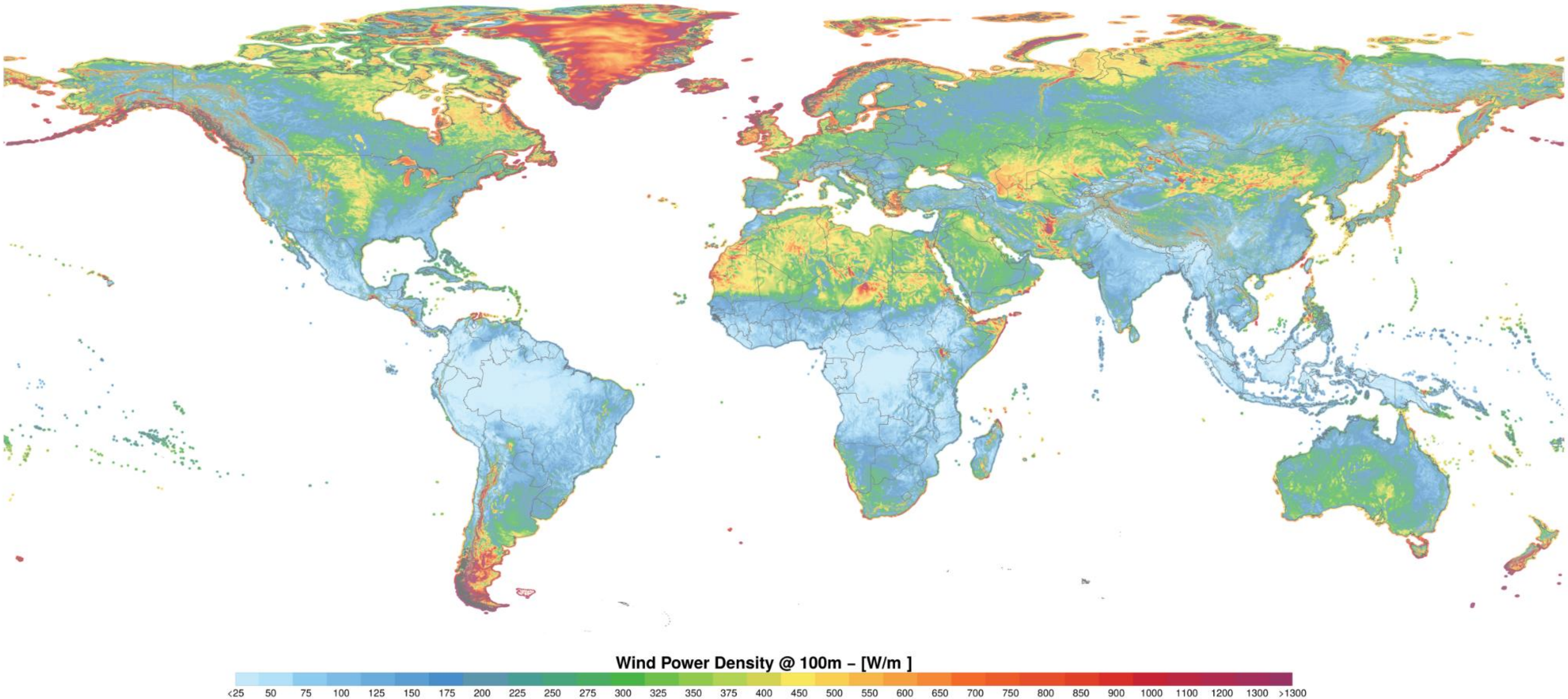

This map is published by the World Bank Group, funded by ESMAP, and prepared by DTU and Vortex. For more information and terms of use, please visit http://globalwindatlas.info

Renewable Electricity in Major Countries, 1991-2021

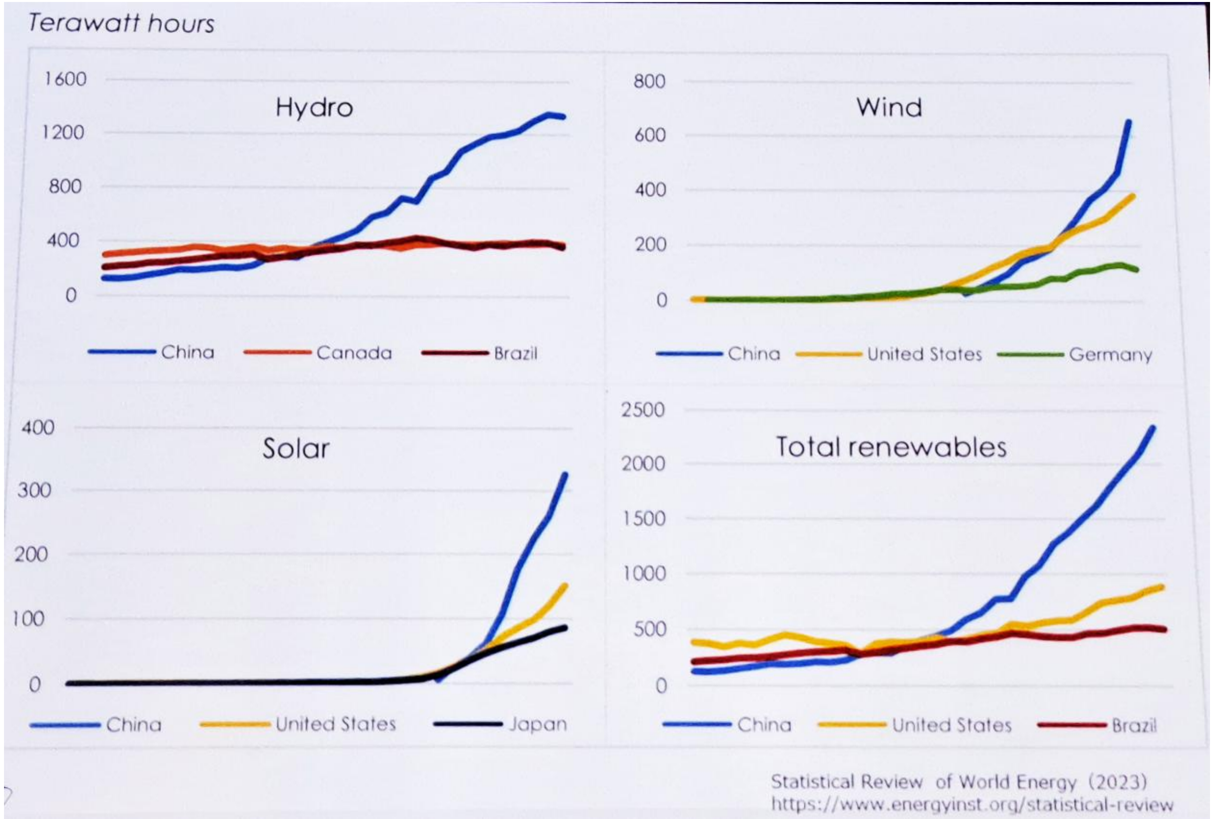

Fluctuating Renewable Energy Sources

Most renewable energy sources have a fluctuating output.

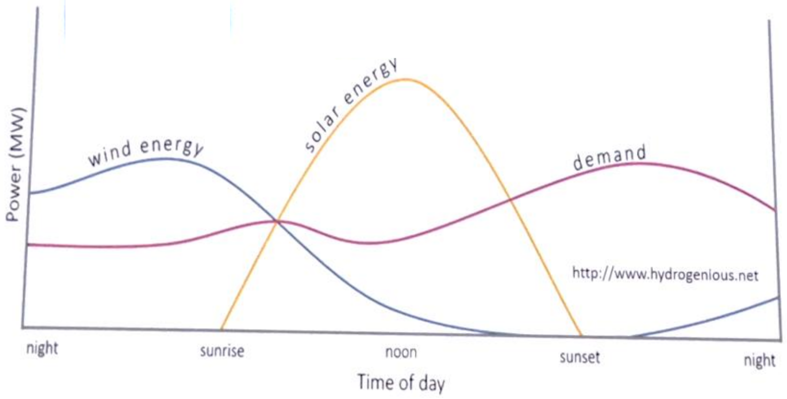

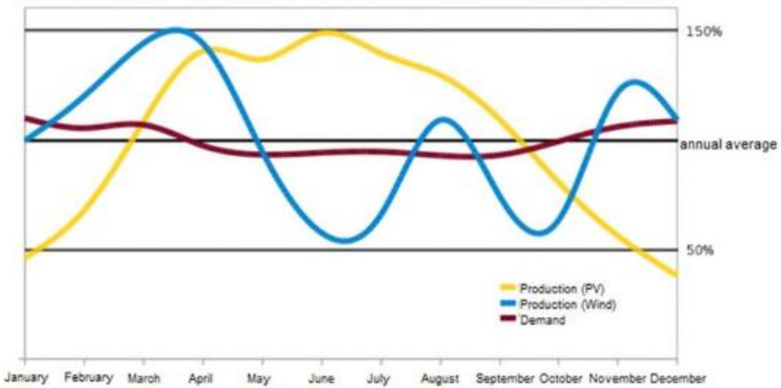

Source: http://michaelwenzl.de/wiki/ee:virtuelles-kraftwerk-lechfeld:vortrag_gruene

Need for storage solutions!

Electric Energy Storage Technologies

Chemical Energy Storage
Hydrogen Storage
Synthetic Fuels

Electrical Storage
Batteries Li-ion, Pb-acid, NaS
Flow batteries
Supercapacitors
Superconducting Magnetic Energy Storage (SMES)

Thermal Energy Storage
Molten Salt Storage
Ice Storage
Sensible and Latent Heat Storage

Mechanical Energy Storage
Pumped Hydroelectric Storage (PHS)
Flywheel Energy Storage (FES)
Compressed Air Energy Storage (CAES)
Gravitricity

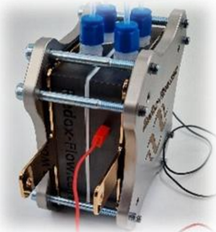

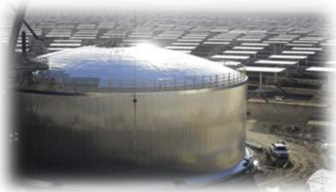

Hydrogen technology

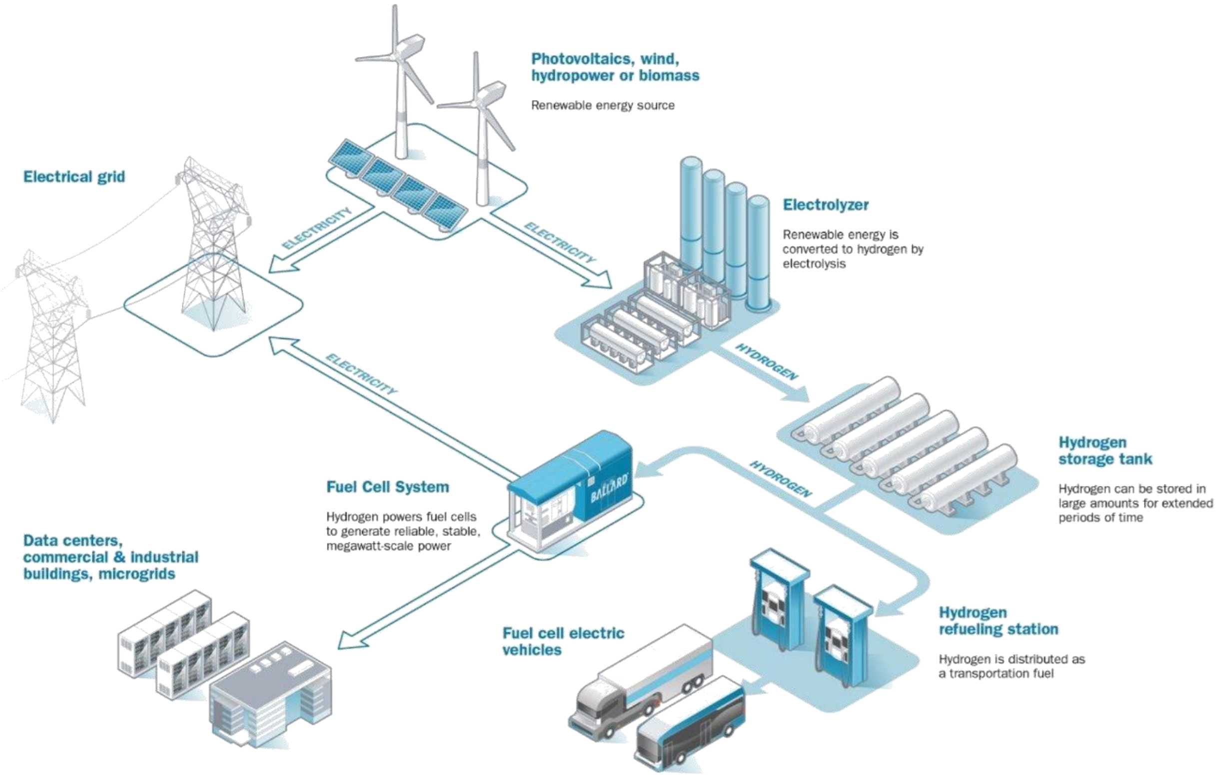

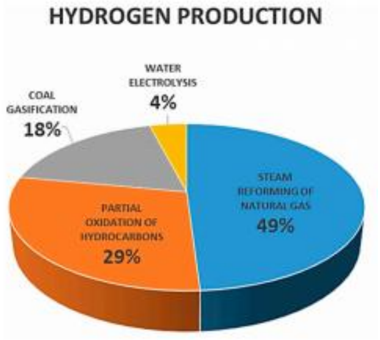

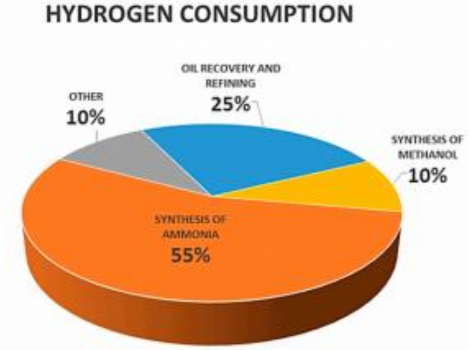

Sdanghi, G.; Maranzana, G.; Celzard, A.; Fierro, V. Towards Non-Mechanical Hybrid Hydrogen Compression for Decentralized Hydrogen Facilities. Energies 2020, 13, 3145

Preparation and testing

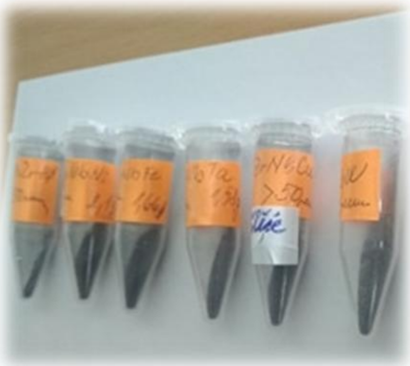

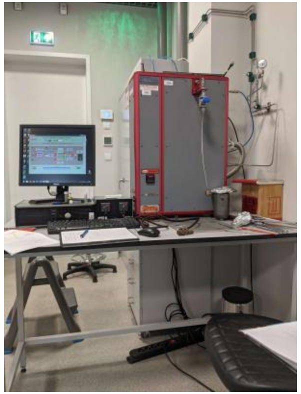

Performance

cooperation with Dr. L.Gondek, AGH Krakow

Hydrogen absorption

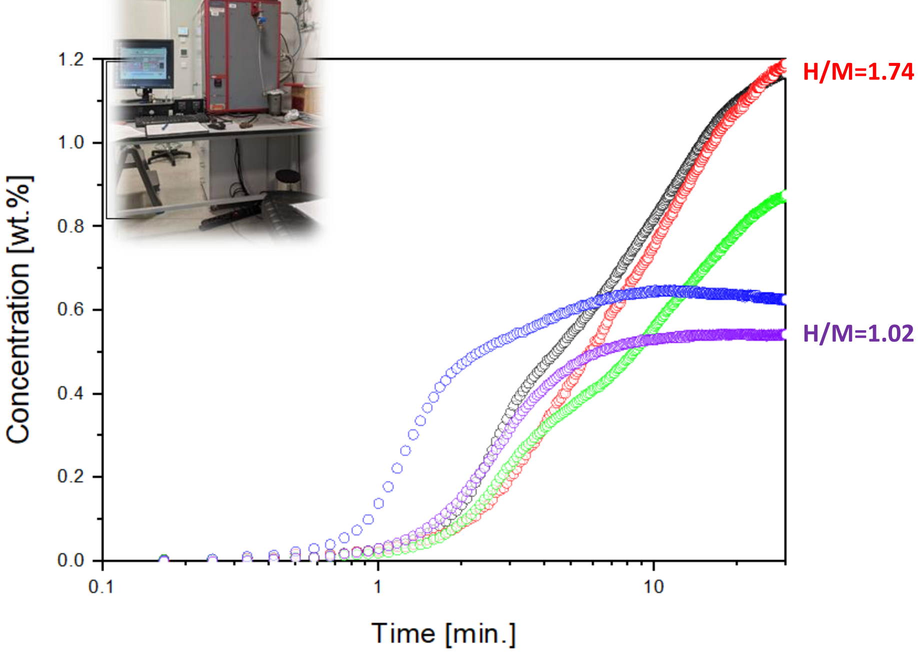

Hydrogen desorption